



# NAVAL POSTGRADUATE SCHOOL

MONTEREY, CALIFORNIA

## THESIS

**ESTIMATION OF GEOACOUSTIC PROPERTIES IN THE  
SOUTH CHINA SEA SHELF USING A TOWED SOURCE  
AND VERTICAL LINE HYDROPHONE ARRAY**

by

John M. Marburger

December 2004

Thesis Advisor:  
Second Reader:

Ching-Sang Chiu  
Chris Miller

**Approved for public release; distribution is unlimited**

THIS PAGE INTENTIONALLY LEFT BLANK

**REPORT DOCUMENTATION PAGE**

Form Approved OMB No. 0704-0188

Public reporting burden for this collection of information is estimated to average 1 hour per response, including the time for reviewing instruction, searching existing data sources, gathering and maintaining the data needed, and completing and reviewing the collection of information. Send comments regarding this burden estimate or any other aspect of this collection of information, including suggestions for reducing this burden, to Washington headquarters Services, Directorate for Information Operations and Reports, 1215 Jefferson Davis Highway, Suite 1204, Arlington, VA 22202-4302, and to the Office of Management and Budget, Paperwork Reduction Project (0704-0188) Washington DC 20503.

<b>1. AGENCY USE ONLY (Leave blank)</b>	<b>2. REPORT DATE</b> December 2004	<b>3. REPORT TYPE AND DATES COVERED</b> Master's Thesis
<b>4. TITLE AND SUBTITLE:</b> Title (Mix case letters) Estimation of Geoacoustic Properties in the South China Sea Shelf Using a Towed Source and Vertical Line Hydrophone Array.		<b>5. FUNDING NUMBERS</b>
<b>6. AUTHOR(S)</b> LT John Marburger		
<b>7. PERFORMING ORGANIZATION NAME(S) AND ADDRESS(ES)</b> Naval Postgraduate School Monterey, CA 93943-5000		<b>8. PERFORMING ORGANIZATION REPORT NUMBER</b>
<b>9. SPONSORING /MONITORING AGENCY NAME(S) AND ADDRESS(ES)</b> N/A		<b>10. SPONSORING/MONITORING AGENCY REPORT NUMBER</b>
<b>11. SUPPLEMENTARY NOTES</b> The views expressed in this thesis are those of the author and do not reflect the official policy or position of the Department of Defense or the U.S. Government.		
<b>12a. DISTRIBUTION / AVAILABILITY STATEMENT</b> Approved for public release; distribution is unlimited.	<b>12b. DISTRIBUTION CODE</b>	

**13. ABSTRACT (maximum 200 words)**

Linear sound sweeps from a towed J15-3 sound source were collected at a moored VLA hydrophone array in the South China Sea during the ASIAEX experiment in May 2001. Measured signals were filtered and pulse compressed. The processed data showed a high signal to noise ratio. Given an *a priori* chirp sonar survey, a two layer bottom "first guess" model was constructed. A broadband coupled-mode model was used to perform an exhaustive frequency variant sensitivity study of VLA pressures to changes in bottom properties as a basis for the geoacoustic inverse problem. Study results provided information on the observability of the various geoacoustic parameters and a procedure for the inversion. Matched field processing of the VLA data, using the same coupled-mode model, was then performed to calculate ambiguity diagrams from which geoacoustic parameter estimates were obtained. Since VLA pressure fields were not sensitive to changes in the sediment attenuation coefficient, a matched field technique that correlated the slope of modeled transmission loss to the negative slope of 10log of the observed energy was performed in order to obtain estimates of the attenuation. These estimates showed a frequency dependent attenuation coefficient in the 50-600Hz frequency band.

<b>14. SUBJECT TERMS</b> Geoacoustic, Inversion, Matched field, South China Sea, Sensitivity		<b>15. NUMBER OF PAGES</b> 49
<b>16. PRICE CODE</b>		
<b>17. SECURITY CLASSIFICATION OF REPORT</b> Unclassified	<b>18. SECURITY CLASSIFICATION OF THIS PAGE</b> Unclassified	<b>19. SECURITY CLASSIFICATION OF ABSTRACT</b> Unclassified
		<b>20. LIMITATION OF ABSTRACT</b> UL

NSN 7540-01-280-5500

Standard Form 298 (Rev. 2-89)  
Prescribed by ANSI Std. Z39-18

THIS PAGE INTENTIONALLY LEFT BLANK

**Approved for public release; distribution is unlimited**

**ESTIMATION OF GEOACOUSTIC PROPERTIES IN THE SOUTH CHINA SEA  
SHELF USING A TOWED SOURCE AND VERTICAL LINE HYDROPHONE  
ARRAY**

John M. Marburger  
Lieutenant, United States Navy  
B.S., United States Naval Academy, 1998

Submitted in partial fulfillment of the  
requirements for the degree of

**MASTER OF SCIENCE IN  
PHYSICAL OCEANOGRAPHY AND METEOROLOGY**

from the

**NAVAL POSTGRADUATE SCHOOL  
December 2004**

Author: John Marburger

Approved by: Ching-Sang Chiu  
Thesis Advisor

Christopher Miller  
Second Reader

Mary Batteen  
Chairman, Department of Oceanography

THIS PAGE INTENTIONALLY LEFT BLANK

## ABSTRACT

Linear sound sweeps from a towed J15-3 sound source were collected at a moored VLA hydrophone array in the South China Sea during the ASIAEX experiment in May 2001. Measured signals were filtered and pulse compressed. The processed data showed a high signal to noise ratio. Given an *a priori* chirp sonar survey, a two layer bottom “first guess” model was constructed. A broadband coupled-mode model was used to perform an exhaustive frequency variant sensitivity study of VLA pressures to changes in bottom properties as a basis for the geoacoustic inverse problem. Study results provided information on the observability of the various geoacoustic parameters and a procedure for the inversion. Matched field processing of the VLA data, using the same coupled-mode model, was then performed to calculate ambiguity diagrams from which geoacoustic parameter estimates were obtained. Since VLA pressure fields were not sensitive to changes in the sediment attenuation coefficient, a matched field technique that correlated the slope of modeled transmission loss to the negative slope of  $10\log$  of the observed energy was performed in order to obtain estimates of the attenuation. These estimates showed a frequency dependent attenuation coefficient in the 50-600Hz frequency band.

THIS PAGE INTENTIONALLY LEFT BLANK

## TABLE OF CONTENTS

I.	INTRODUCTION.....	1
A.	ASIAEX OVERVIEW.....	1
B.	BOTTOM MODEL .....	3
C.	THESIS OBJECTIVES.....	4
D.	THESIS OUTLINE.....	5
II.	SENSITIVITY STUDY .....	7
A.	SENSITIVITY STUDY DETAILS.....	7
B.	STUDY RESULTS.....	9
1.	Thin Layer .....	9
2.	Bottom Layer.....	15
III.	DATA INVERSION.....	19
A.	MATCHED FIELD PROCESSING .....	19
B.	ESTIMATOR DESIGN.....	20
C.	THIN LAYER INVERSION.....	21
C.	BOTTOM LAYER INVERSION.....	24
D.	ATTENUATION INVERSION .....	26
IV.	CONCLUSIONS .....	31
LIST OF REFERENCES.....		33
INITIAL DISTRIBUTION LIST .....		35

THIS PAGE INTENTIONALLY LEFT BLANK

## LIST OF FIGURES

Figure 1.	ASIAEX experiment location (shown in red box) relative to China and Taiwan coastlines situated on continental shelf/slope. Bathymetry is indicated by contours.....	1
Figure 2.	J-15 source signals used for geoacoustic inversion. Black arrows indicate low, mid and high frequency sweeps at 50-200 Hz, 240-260 Hz and 550-600 Hz respectively.....	2
Figure 3.	J-15 ship track (bottom) and range from VLA (top). Thin black arrows show the direction of ship movement. Green dot is the range (5km) where vertical measured data (black dot) for the matched field processing was gathered. Black x's are the ranges used for horizontal data applied to the attenuation inversion only.....	3
Figure 4.	Across shelf chirp sonar image of bottom bathymetry for ASIAEX location. The VLA receiver is located at the 124m isobath and is marked by a black pentagon. ....	4
Figure 5.	Thin Layer Sound Speed Sensitivity. Frequency increases from 50Hz at the top left to 575Hz at the bottom right. Frequency on diagrams increase left to right and top to bottom. Colorbar ranges from zero to one and represents correlation values. Sound speed increments range from 1550 to 1650 m/s.....	10
Figure 6.	Thin Layer Density Sensitivity. Frequency increases from 50Hz at the top left to 575Hz at the bottom. Frequency on diagrams increase left to right and top to bottom. Colorbar ranges from zero to one and represents correlation values. Lack of contours shows insensitivity of VLA pressure to bottom density fluctuations.....	11
Figure 7.	Thin Layer Attenuation Sensitivity. Frequency increases from 50Hz at the top left to 575Hz at the bottom. Frequency on diagrams increase left to right and top to bottom. Colorbar ranges from zero to one and represents correlation values. Lack of contours shows insensitivity of VLA pressure to bottom attenuation fluctuations .....	12
Figure 8.	Thin layer attenuation sensitivity via TL slopes of modeled data. Subplots are for low, mid and high LFM sweeps. Frequencies increase from top (125Hz) to bottom (575Hz). Changing slopes show that TL slope is sensitive to $\alpha$ and that range aperture is required to estimate $\alpha$ .....	13
Figure 9.	Thin Layer Thickness Sensitivity. Frequency increases from 50Hz at the top left to 575Hz at the bottom. Frequency on diagrams increase left to right and top to bottom. Colorbar ranges from zero to one and represents correlation values. Thickness increments range from 2 to 20 meters.....	14
Figure 10.	Bottom Layer Sound Speed Sensitivity (Low Frequencies). Frequency increases from 50Hz at the top left to 140Hz at the bottom right. Frequency on diagrams increase left to right and top to bottom. Colorbar	

	ranges from zero to one and represents correlation values. Sound speed increments range from 1610 to 1750 m/s. ....	16
Figure 11.	Bottom Layer Sound Speed Sensitivity (Low Frequencies). Frequency increases from 150Hz at the top left to 575Hz at the bottom. Frequency on diagrams increase left to right and top to bottom. Colorbar ranges from zero to one and represents correlation values. Sound speed increments range from 1610 to 1750 m/s. ....	17
Figure 12.	Thin layer ambiguity diagrams for both sound speed and layer thickness. Frequency increases from 140Hz at the top left to 180Hz at the bottom right. Frequency on diagrams increase left to right and top to bottom. Colorbars are not constant for each subplot with darkest red representing max correlation coefficient values for each diagram. Sound speed varies from 1550 to 1650 m/s while layer thickness ranges from 2 to 20 meters. ....	23
Figure 13.	Low frequency LFM amplitude spectrum after pulse compression showing obvious peaks in SNR that were used for bottom sound speed inversion in Figure 13. ....	25
Figure 14.	Bottom layer sound speed frequency dependent ambiguity diagram with sound speed ranging from 1590 to 1730 m/s. Highest correlation coefficients are depicted in reds and oranges and correspond to estimated sound speeds on y axis. ....	25
Figure 15.	LFM measured negative energy (-10logE) slopes for low (50-200Hz), mid (240-260 Hz) and high (550-600 Hz) sweeps relative to energy at 4km. ....	27
Figure 16.	Attenuation ambiguity diagrams. Top subplot is for 125Hz, middle is 250Hz and bottom is 575Hz. X axis represents the attenuation value estimated from its corresponding TL slope. The y axis is the correlation coefficient value. ....	28
Figure 17.	Attenuation rate versus frequency. Data set fit with a cubic spline curve. ....	29

## **ACKNOWLEDGMENTS**

First, I would like to thank Professor Ching-Sang Chiu, for giving me the guidance that I needed to make this a worthwhile study. Although I am his 46<sup>th</sup> masters' student and one of his professed last, I imagine that exceptions could be made with some coercion.

Of the utmost importance to this study was Chris Miller. It is doubtful that this thesis would have been finished without his tutelage in the areas of data mining and signal processing. He has made the process enjoyable. As an additional bonus, he has become a valued friend and I wish him and his beloved Pippen all the happiness that is possible.

And lastly, I wish to thank my wonderful wife for her love and support. She has given up her promising career so that I can follow mine and I am deeply in her debt.

THIS PAGE INTENTIONALLY LEFT BLANK

## I. INTRODUCTION

### A. ASIAEX OVERVIEW

The Asian Seas International Acoustics Experiment (ASIAEX) was a joint scientific experiment between the United States, China, Korea and Taiwan (Chiu *et al.*, 2004). Institutions in the United States included the Naval Postgraduate School, Naval Research Laboratory and Woods Hole Oceanographic Institution. The study was multi-faceted but was primarily focused on exploring the predictability of low frequency sound propagation along/across the shelf break in the South China Sea and the effect of ocean variability upon that predictability (Ramp *et al.*, 2004). The prediction required a characterization of geoacoustic parameters and is the focus of this paper.

The experiments were performed in April-August 2001 in the region of the South China Sea (Figure 1). Data used in this study was gathered on May 5<sup>th</sup> 2001. This day was specifically chosen for its minimal water column variability (Chiu *et al.*, 2004).

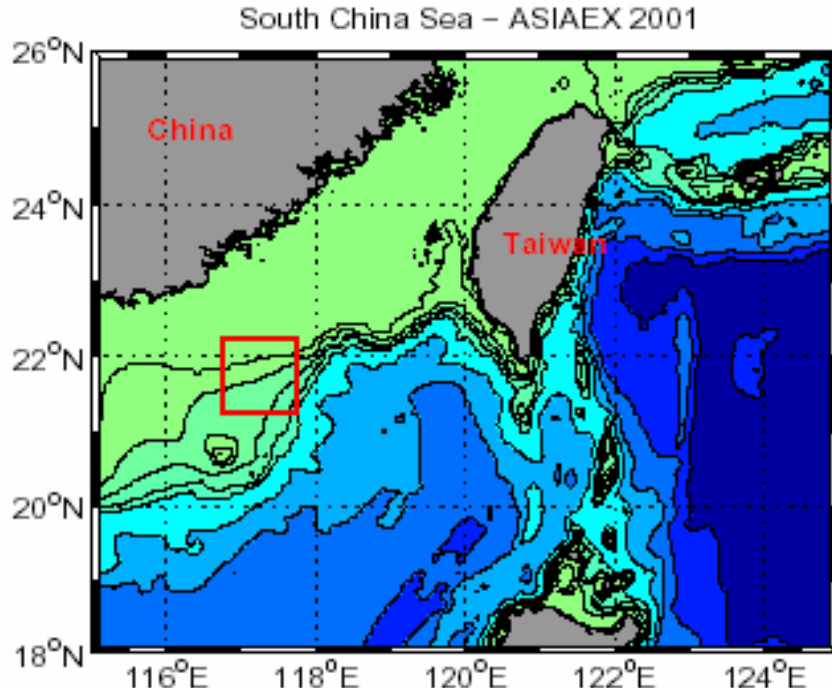


**Figure 1.** ASIAEX experiment location (shown in red box) relative to China and Taiwan coastlines situated on continental shelf/slope. Bathymetry is indicated by contours.

The acoustic source of this data was a J-15-3 broadband source towed behind the R/V Ocean Researcher III (OR3) at a speed of 2 knots and a depth of 3 meters. A variety of waveforms were broadcast including a linear frequency modulated (LFM) sweep ensemble used for this experiment (Figure 2). The LFM sweeps were broadcast continuously over 12 hours. Each thirty second ensemble was broken into three ten second sweeps with low, mid and high broadcasts of 50-200 Hz, 240-260 Hz, and 550-600 Hz hereafter referred to as LF, MF and HF respectively. A 10% cosine window was applied to the LFM waveform to properly ramp up amplitude. The frequencies chosen were specifically designed not to overlap in frequency with signals from moored sources that were broadcasting simultaneously (Turgut *et al.*, 2003).

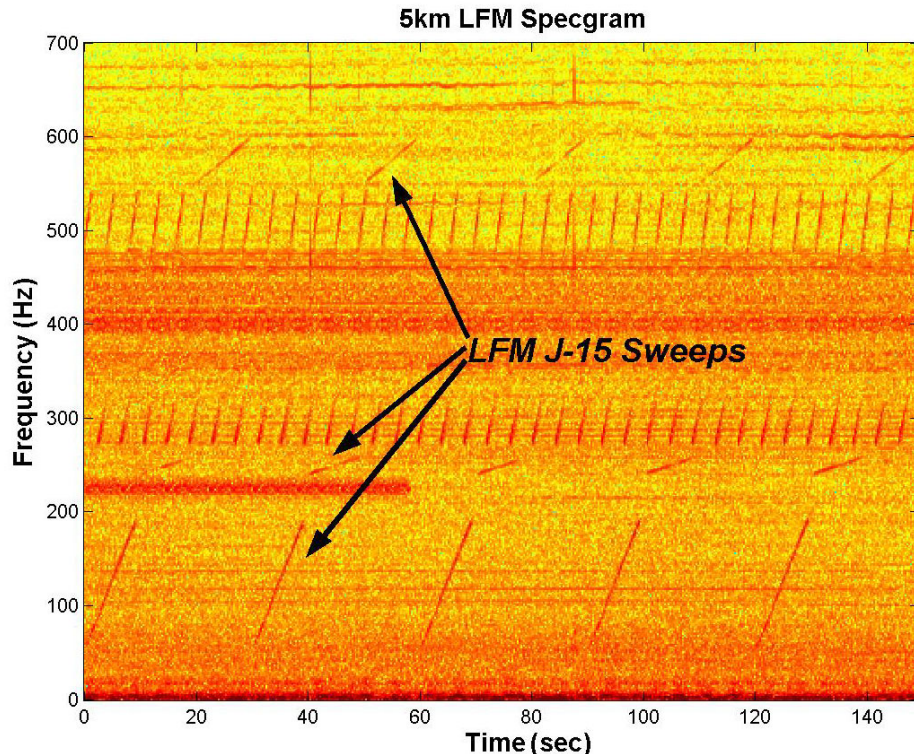


**Figure 2.** J-15 source signals used for geoacoustic inversion. Black arrows indicate low, mid and high frequency sweeps at 50-200 Hz, 240-260 Hz and 550-600 Hz respectively.

Received acoustic data was recorded on a moored hydrophone vertical line array (VLA) housed on an instrument sled in 124 meters of water. Hydrophone spacing on the VLA was set at 3.75 meters in order to adequately cover most of the water column with

its 16 elements. Data was continuously recorded over the entire duration of the towed-source operation with the ship track shown in Figure 3.

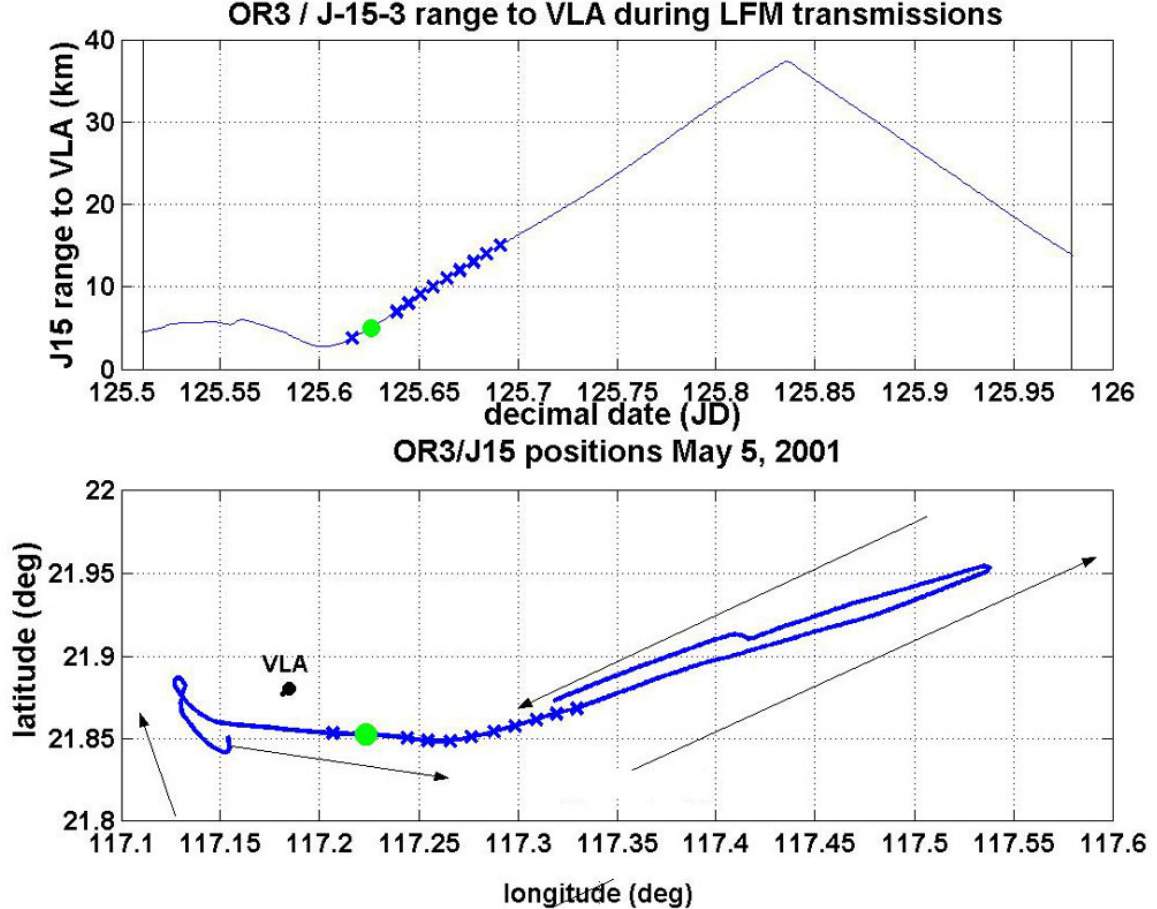


**Figure 3.** J-15 ship track (bottom) and range from VLA (top). Thin black arrows show the direction of ship movement. Green dot is the range (5km) where vertical measured data (black dot) for the matched field processing was gathered. Black x's are the ranges used for horizontal data applied to the attenuation inversion only.

## B. BOTTOM MODEL

The environmental bottom model structure used for both the sensitivity study and matched field processing was obtained by examining the chirp sonar survey imagery obtained by Steve Schock during ASIAEX (Schock, 2004). Visual analysis shows a simple two layer bottom structure, a thin sediment layer overlaying a thicker bottom layer, on the continental shelf and slope. This paper is focused only on the shelf as the

acoustic path from the towed source to the VLA never crossed more than a 20 meter change in bathymetry.

While the chirp data provided the two layer structure of the bottom model (Figure 4), core samples performed during ASIAEX provided a “first guess” sediment classification of the top meter of the bottom. Empirical and regressive equations obtained by Hamilton (1980) based on historical, world wide data were used to provide rough sound speed, density (Hamilton, 1977) and attenuation values given sediment type. Results from a previous inversion (Lin *et al.* 2001) in the same area but using a lower frequency broad band source from dynamite fishing were checked against the Hamilton data and, if reasonable, were used as first guess nominal values.

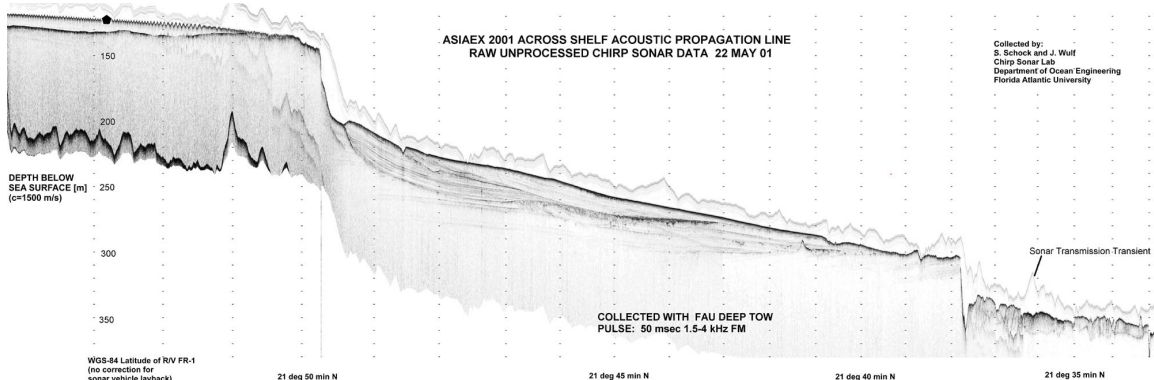


**Figure 4. Across shelf chirp sonar image of bottom bathymetry for ASIAEX location. The VLA receiver is located at the 124m isobath and is marked by a black pentagon.**

Bottom parameters in question, in each layer, are sound speed, attenuation and density. Given the two layer nature displayed by the chirp sonar, thin layer thickness becomes the seventh and final parameter, four in the thin layer and three in the bottom.

### C. THESIS OBJECTIVES

The sonar operator with a detailed understanding of acoustic propagation and the environmental parameters that affect it carries a significant advantage over an adversary with all other factors equal. Therefore, the overall objective of this thesis is to provide

the warfighter with information critical to undersea warfare. As the typical naval operational environment migrates from open ocean “blue water” to littoral shallow water locales, an adequate characterization of the complex bottom environment is critical to the accurate prediction of acoustic propagation. The quantification of bottom characteristics in the experiment region via an inverse method is a means to help achieve the goal of warfighter support, in this case, to process the VLA data to obtain reliable estimates of the geoacoustic parameters. To ensure a sound scientific answer for the inversion, a sensitivity study is needed to determine the observability of acoustically significant parameters in the bottom, the quality of the inversion and the formulation for the inverse procedure.

#### **D. THESIS OUTLINE**

To accomplish the thesis objectives, the investigation into sensitivity of VLA pressure fields to bottom parameters was modeled first. Model runs were executed for each of the parameters in question. Results were cross-correlated to show vertical sound field sensitivity to each of the parameters, inversion quality and the information to develop a procedure for the inversion.

With the sensitivity study completed, the model was again run to produce multiple VLA fields for matched field processing using the study findings as guidelines. Modeling was performed by the same coupled modes model.

Details and results of the sensitivity study are presented in Chapter II. Chapter III explains the inverse technique and presents results of the geoacoustic parameter estimates. Conclusions and recommendations for further study are presented in the final chapter.

THIS PAGE INTENTIONALLY LEFT BLANK

## II. SENSITIVITY STUDY

### A. SENSITIVITY STUDY DETAILS

The technique of matched field processing is not new to the scientific community or acousticians in general. For several decades this technique has been used extensively on a variety of candidate parameters for different regions (Lynch *et al.*, 1990). What many papers fail to explore prior to performing matched field processing is the sensitivity of the modeled data output to changes in the candidate parameters. This is explored by the creation of a sensitivity diagram which shows the correlation coefficients of a large number of pressure fields generated by incremental changes in a candidate parameter. If little change is observed in output correlation coefficients given a large range of inputs, then the inversion is useless as a reasonable ambiguity diagram cannot be determined.

Sensitivity of the model output also provides insight into the quality of the inversion. The narrowness of the peak in the sensitivity diagram describes the resolvability of the given candidate parameter and the accuracy that a matched field estimation can produce. The most important use for the sensitivity study is the information it provides allows for the development of an efficient inversion. Results from the sensitivity help determine which parameter is inverted for first, second and so on.

The sensitivity study was performed using a broad band coupled modes model developed by Chiu (1996). This is the same model that was used for the matched field processing of the real data with the corresponding results presented in Chapter III.

Seven parameters provided the scope of the sensitivity study.

1. Thin layer sound velocity,  $c$  ( $m/s$ )
2. Bottom layer sound velocity,  $c$  ( $m/s$ )
3. Thin layer density,  $\rho$  ( $kg/m^3$ )
4. Bottom layer density,  $\rho$  ( $kg/m^3$ )
5. Thin layer attenuation,  $\alpha$  ( $dB/km/kHz$ )

6. Bottom layer attenuation  $\alpha$  ( $dB / km / kHz$ )
7. Thin layer thickness,  $h$  ( $m$ )

The ranges and step increments for the candidate parameters were selected based on empirical results from Hamilton (1980) and a similar inversion performed in the same region but at lower frequency by Lin et al. (2001). The prior inversion was used as a basis for the parameter center values. Uncertainty ranges for each parameter were also garnered from the prior inversion but were expanded to ensure that all possible values were explored in the study. The empirical results obtained by Hamilton were used as a quality control.

Each parameter was studied by holding the others constant while the one in question was varied over a given step increment. Bathymetry for the model was input as a flat bottom. Since the slope of the bathymetry was so gradual, a flat bottom simplified the model runs without affecting the results. Hydrophone receiver depths and source depth inputs matched the reported depths exactly.

Frequency was varied for each parameter. Initially, the center frequency of each ASIAEX J-15 sweep was used (125, 250 and 575 Hz). However, the frequency range and increment changed for certain parameters as the initial center frequencies showed weak sensitivity or none at all. This was most noticeable in the MF and HF J-15 frequency sweeps. Since the low sweep had the broadest frequency band and the greatest ability to penetrate the bottom, much information was gathered at these frequencies and necessitated a broader sensitivity study.

Model output of the VLA pressure field was used for the sensitivity study. Pressure output was demeaned vertically and normalized to have the sum of the squares equal to unity. The output was then correlated to the conjugate transpose of pressure fields produced by incrementally changing the parameter to be studied. Calculated cross correlation coefficients were then contoured to give the sensitivity diagram.

## B. STUDY RESULTS

### 1. Thin Layer

The thin layer is characterized by four parameters. It would be ideal if a frequency band existed that only showed sensitivity to the upper thin layer and none in the lower layer. If no frequency of that type could be found, the inversion would be much more computationally demanding.

The first thin layer parameter examined was sound speed. Values varied from 1550 to 1650 m/s with an increment of 5 m/s. Results showed weak sensitivity in the lower bounds of the low frequency sweep (50-75 Hz) as evidenced by the high correlation coefficient values with large standard deviations (wide peaks). Good sensitivity, shown by high correlation coefficients with small standard deviations, that improved with increasing frequency were observed for the rest of the frequency range (Figure 5).

Values for density varied from 1520 to 1720 by  $5 \text{ kg/m}^3$  increments. Results were poor with no sensitivity showing for the thin layer (Figure 6).

Attenuation values were varied between .1 and .35 by .025 dB/km/kHz increments. In prior inversions (Rajan *et al.*, 1987) using a normal modes model, attenuation was not invertible so it was expected that attenuation fluctuation over a large range of inputs would not produce any sensitivity in the pressure fields. The results matched expectations (Figure 7). Attenuation would therefore need to be estimated via a different method. Instead of using VLA pressures, pressure vs. range outputs from the BBCM model were used to calculate TL. Figure 8 shows that slopes of the TL are sensitive to  $\alpha$ . Vertical information is therefore not useful, but a range aperture is required for estimation of  $\alpha$ .

The final parameter for the thin layer was thickness. The input model values ranged from 2 to 20 meters every one meter. Results (Figure 9) showed moderate but acceptable sensitivity in the lower portions of the low sweep (50-75 Hz). Excellent sensitivity at the center frequency of the low sweep was observed. The mid to high frequency sweeps had poor sensitivity.

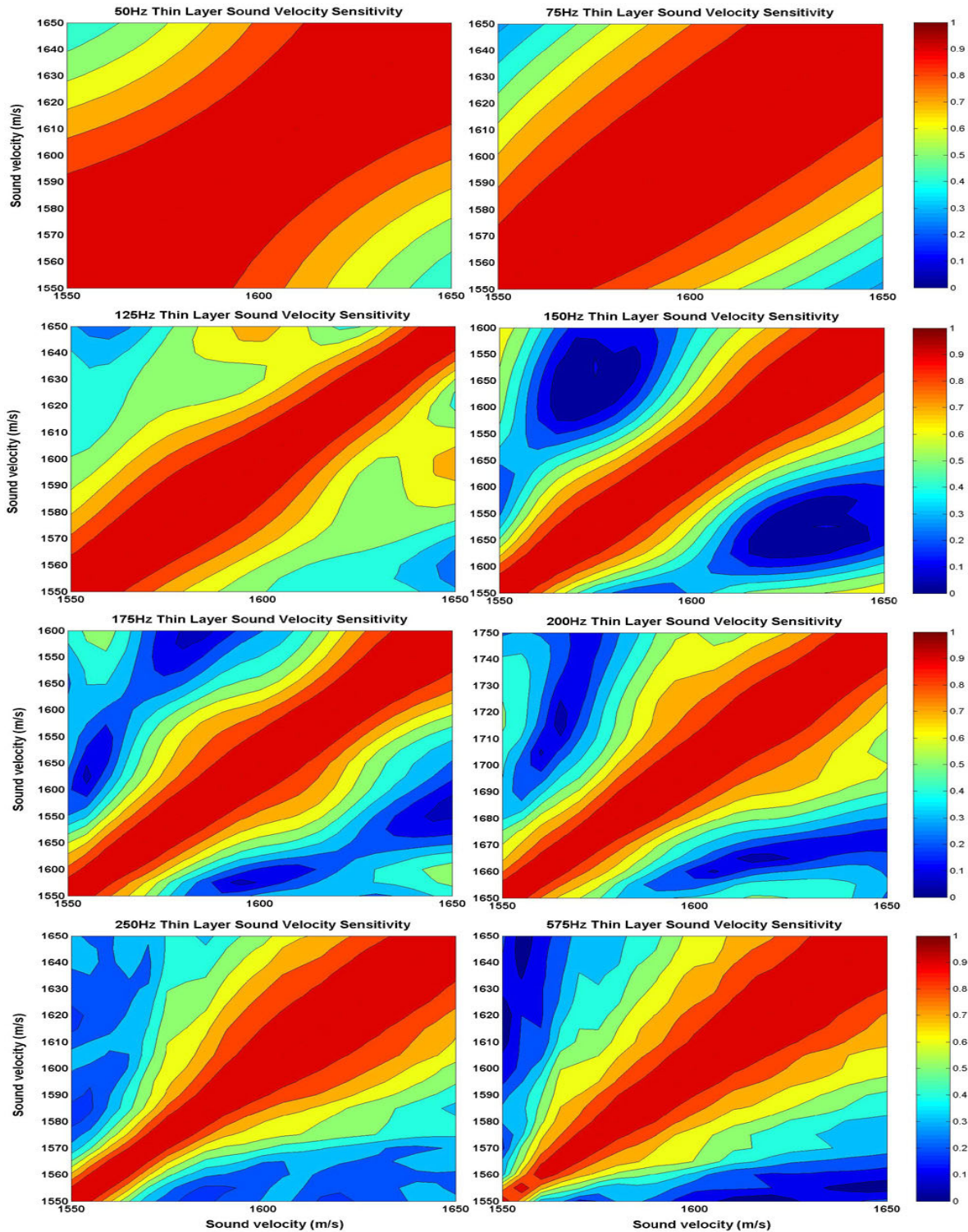


**Figure 5. Thin Layer Sound Speed Sensitivity.** Frequency increases from 50Hz at the top left to 575Hz at the bottom right. Frequency on diagrams increase left to right and top to bottom. Colorbar ranges from zero to one and represents correlation values. Sound speed increments range from 1550 to 1650 m/s.

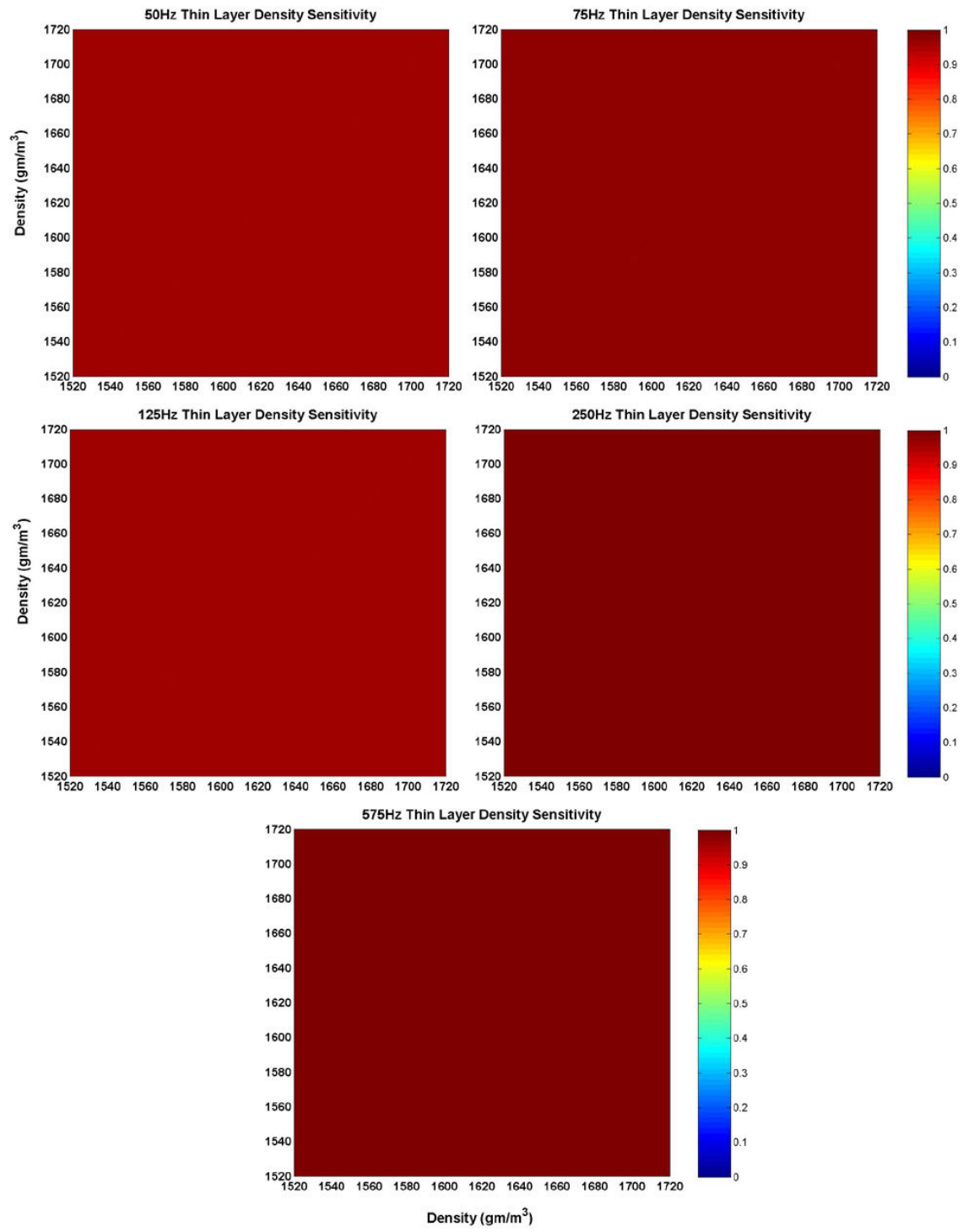


**Figure 6. Thin Layer Density Sensitivity. Frequency increases from 50Hz at the top left to 575Hz at the bottom. Frequency on diagrams increase left to right and top to bottom. Colorbar ranges from zero to one and represents correlation values. Lack of contours shows insensitivity of VLA pressure to bottom density fluctuations.**

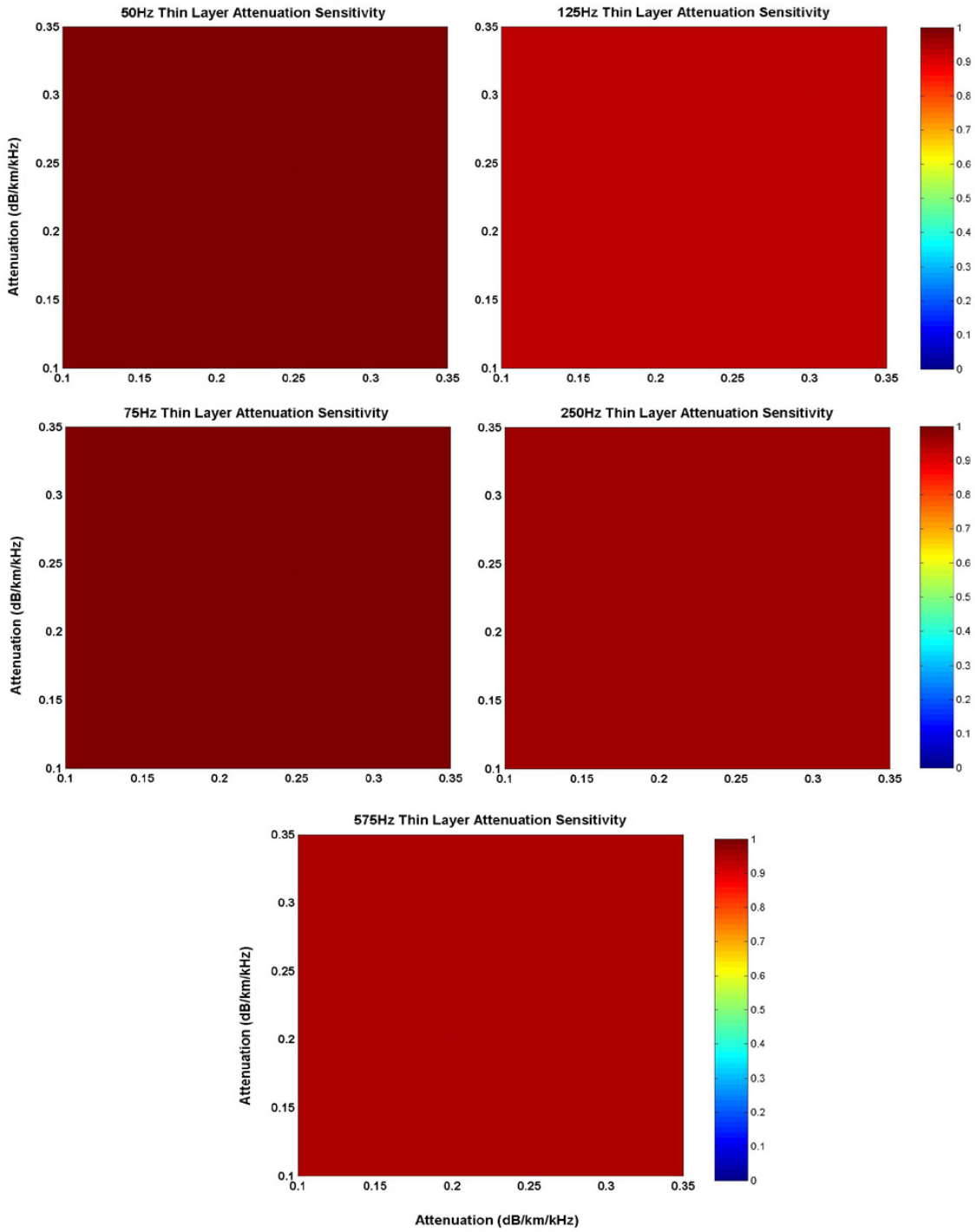


**Figure 7. Thin Layer Attenuation Sensitivity. Frequency increases from 50Hz at the top left to 575Hz at the bottom. Frequency on diagrams increase left to right and top to bottom. Colorbar ranges from zero to one and represents correlation values. Lack of contours shows insensitivity of VLA pressure to bottom attenuation fluctuations**

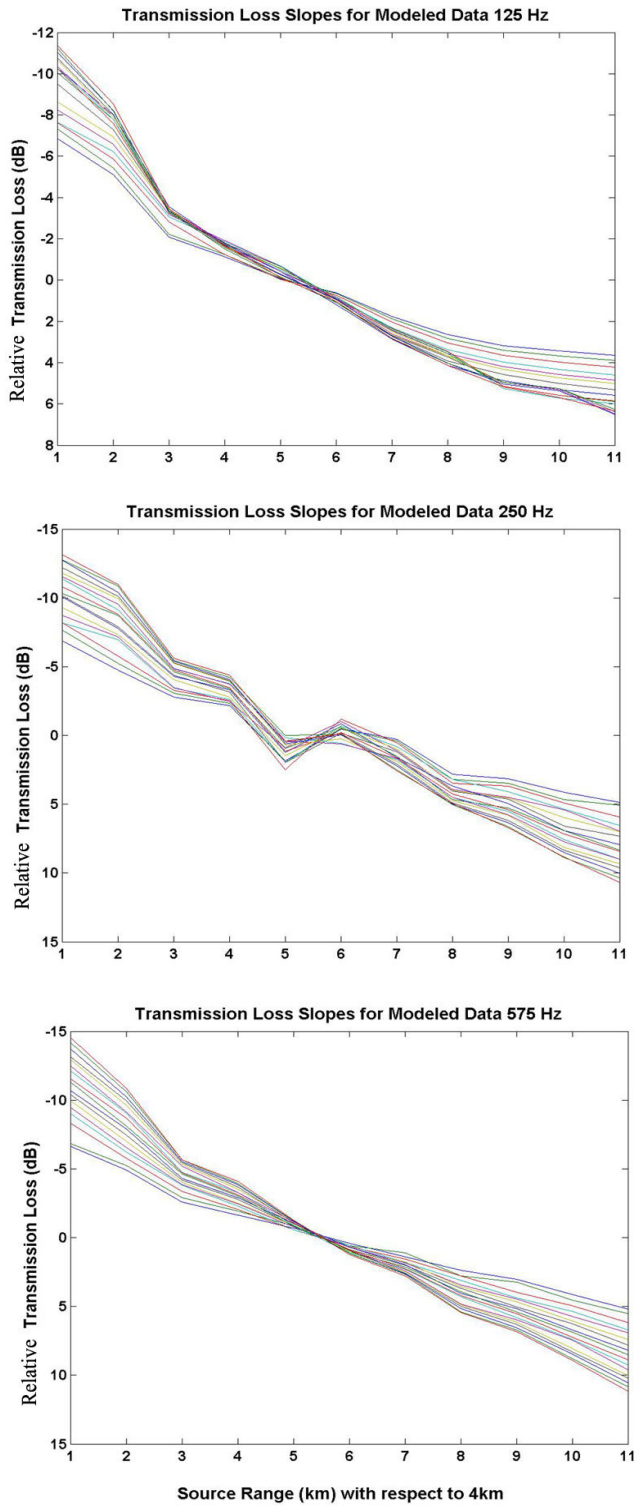


**Figure 8.** Thin layer attenuation sensitivity via TL slopes of modeled data.  
 Subplots are for low, mid and high LFM sweeps. Frequencies increase from top (125Hz) to bottom (575Hz). Changing slopes show that TL slope is sensitive to  $\alpha$  and that range aperture is required to estimate  $\alpha$ .

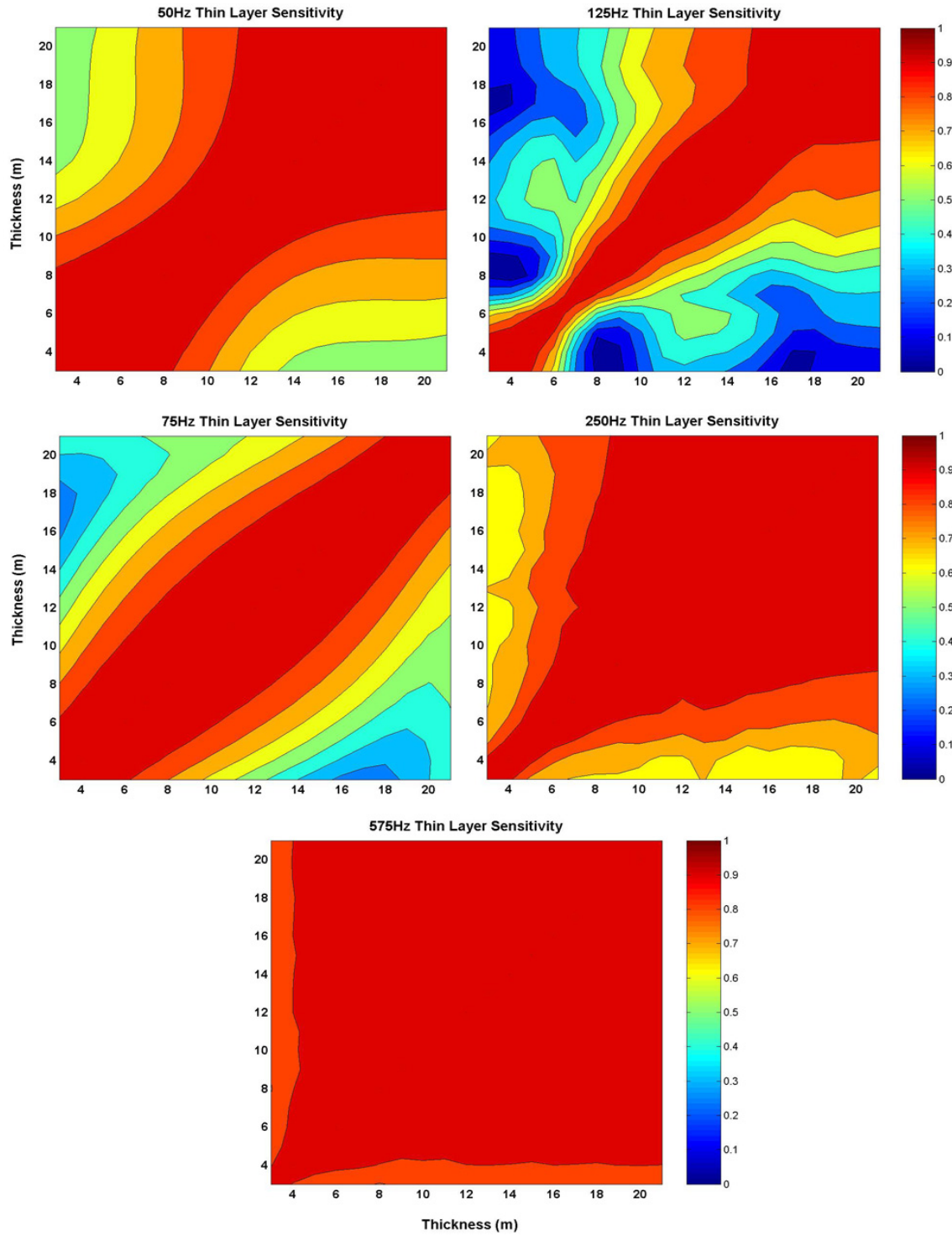


**Figure 9. Thin Layer Thickness Sensitivity.** Frequency increases from 50Hz at the top left to 575Hz at the bottom. Frequency on diagrams increase left to right and top to bottom. Colorbar ranges from zero to one and represents correlation values. Thickness increments range from 2 to 20 meters.

## **2. Bottom Layer**

Visual inspection of the chirp sonar image showed the thin sediment layer covering the bottom layer to be at least 10 meters thick. This thickness is important number as penetration depth of the sound is a function of frequency. A 50 Hz signal (~30 meter wavelength) can penetrate approximately 50 meters (Lin *et al.* 2001) with less penetration as frequency increases. The hypothesis was that the bottom layer would therefore be sensitive to the lower frequencies only.

Parameter values were varied between 1610 and 1750 m/s by an increment of 5 m/s. As expected, increased sensitivity was observed at the lower frequencies, especially in the lower portion of the low sweep (Figure 10). Poor or no sensitivity was seen above 140 Hz (Figure 11) as the wavelengths became smaller than 11m.

Attenuation and density showed similar poor sensitivity results in the bottom layer as in the thin layer. The graphical results were omitted in the interest of space and repetition for this paper. The results are identical to the thin layer density and attenuation graphics in Figures 6 and 8.

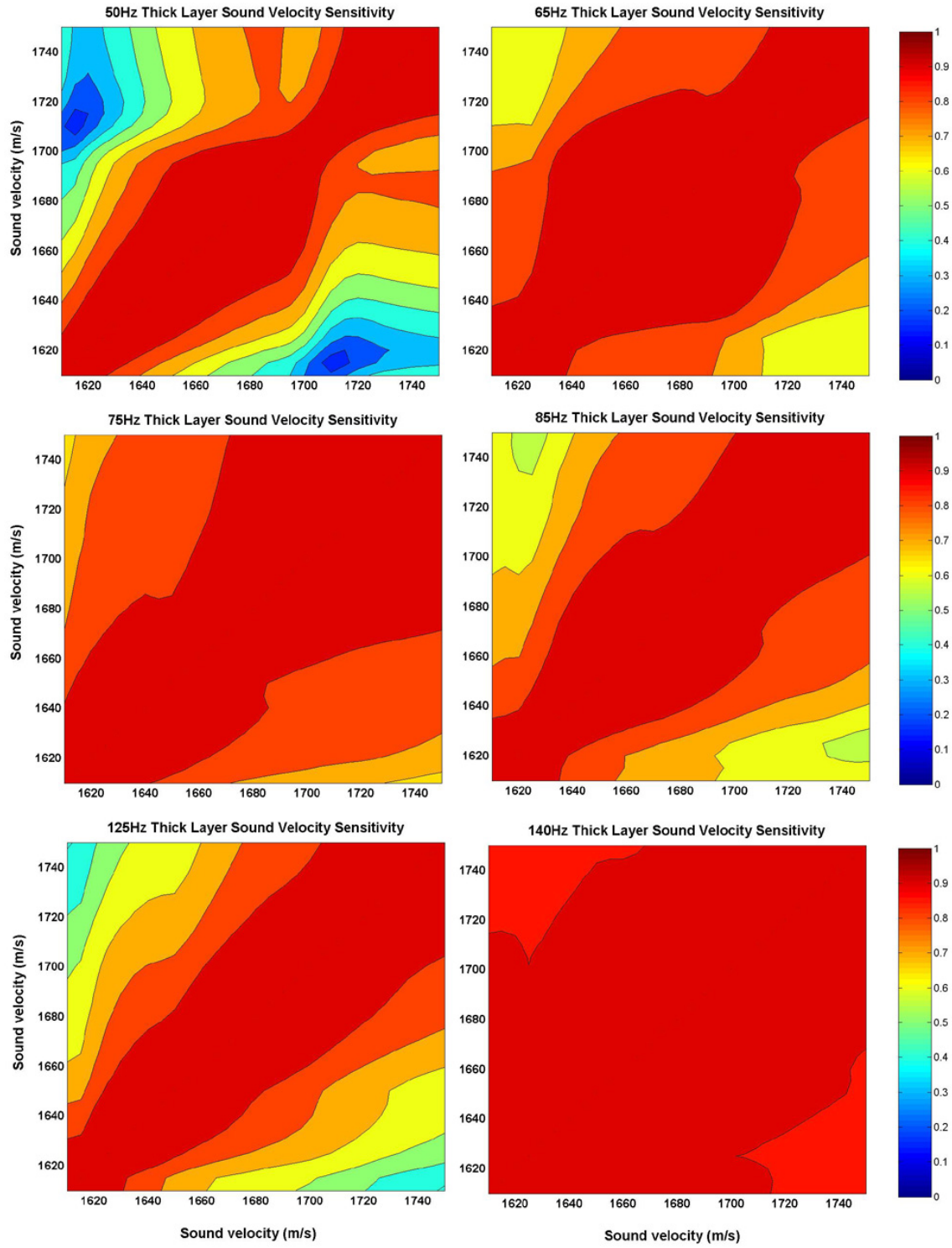


**Figure 10. Bottom Layer Sound Speed Sensitivity (Low Frequencies).** Frequency increases from 50Hz at the top left to 140Hz at the bottom right. Frequency on diagrams increase left to right and top to bottom. Colorbar ranges from zero to one and represents correlation values. Sound speed increments range from 1610 to 1750 m/s.

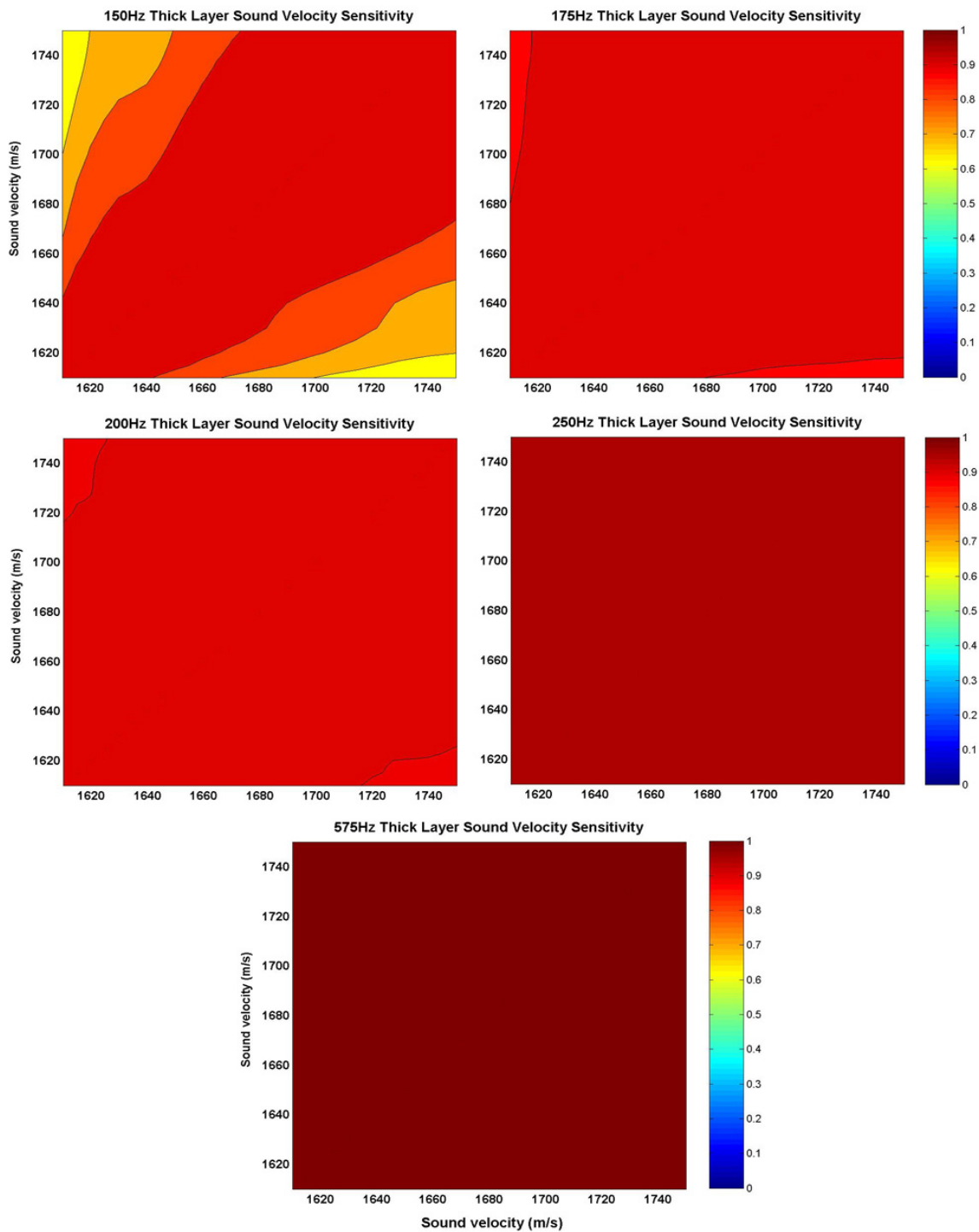


**Figure 11. Bottom Layer Sound Speed Sensitivity (Low Frequencies).** Frequency increases from 150Hz at the top left to 575Hz at the bottom. Frequency on diagrams increase left to right and top to bottom. Colorbar ranges from zero to one and represents correlation values. Sound speed increments range from 1610 to 1750 m/s.

THIS PAGE INTENTIONALLY LEFT BLANK

### **III. DATA INVERSION**

#### **A. MATCHED FIELD PROCESSING**

Matched field processing (MFP) has quickly become one of the most popular and widely used signal processing techniques for acoustics. The popularity is due to its ability to handle a wide range of problems that often confront acousticians in their investigations. Matched field is ideal for studies to determine parameters that affect the propagation of sound (Tolstoy, 1993), which is the goal of this paper. MFP also works well for localization type problems as well as model studies, again touched upon in this paper during the sensitivity study in Chapter II.

Matched field does have its limitations. Noise is the enemy of MFP as is an ocean environment that is temporally variable during the period of data gathering (Tolstoy, 1993). . The J-15 propagation experiment occurred over 3 days, however, only the May 5<sup>th</sup> data was used in this study as it was the most stable.

As the field of MFP has progressed, numerous modifications have been added to improve results based on the variables in a given experiment. Processors have certain advantages over others. Resolution, sidelobes, and model errors are all handled differently with tradeoffs from processor to processor (Tolstoy, 1993).

This study uses a linear (Bartlett) processor. It is the simplest and most understood of the processors available. It handles model inaccuracies and perturbations well and was a good choice for the study. Although sidelobes (regions of erroneous high processor power) are often associated with this processor (Tolstoy, 1993), they did not prove to be a problem.

The concept behind the processor is simple. It correlates directly measured data with modeled data, in this case measured and modeled pressure fields. Processor power is defined as:

$$C(\underline{x}) = \underline{p}^M (\underline{p}^o \underline{p}^{o^+}) \underline{p}^M,$$

where  $\underline{p}^M$  is the modeled VLA pressure field,  $\underline{p}^o$  is the observed VLA pressure field and  $\underline{p}^+$  is the conjugate transpose of  $\underline{p}$ . Note that these are column vectors of 16x1 elements and correspond to the 16 hydrophones in the VLA.

Prior to entering the data into this linear correlator, both modeled and observed data was respectively normalized to have unit energy (sum of squares equal to one), except for the normalization for the attenuation discussed in detail below.

Raw observed data was sampled every kilometer from 4 to 15 km. At each distance, 150 seconds of data were gathered (Figure 3.). As the LFM sweep ensemble was thirty seconds in duration, each range sample point had five LFM sweeps included. LF, MF and HF sweeps, each 10 seconds long, were combined into usable vectors. Data was then band-pass filtered and pulse compressed to further increase signal to noise ratio (SNR). Pulse compression used a synthetic replica signal to match each J-15 transmission which included the 10% cosine taper used in the experiment. SNR was more than adequate after pulse compression for most frequencies. However, the cosine taper reduced the initial and final 5% of the observed signal which resulted in some SNR issues in the bottom layer inversion. The issue was resolved by choosing frequencies away from the edges of the linear sweep.

## B. ESTIMATOR DESIGN

The final results from the sensitivity study showed that changes in three of the seven candidate parameters produce significant changes in the VLA sound pressures. The study also showed that relatively small (5%) changes in those parameters produced noticeable changes in pressure and would therefore produce an acceptable quality inversion. Most importantly, the study revealed information critical for formulation of the inverse procedure and is as follows:

1. Invert for thin layer sound speed and thin layer thickness first.  
Frequencies used for the inversion should be between 140-200 Hz as

frequencies lower than that showed sensitivity to the bottom layer sound speed as well.

2. Next, invert for bottom layer sound speed. Bandwidth acceptable for inversion is between 65-140 Hz. Signals with frequencies above 130 Hz have wavelengths too short to penetrate deep enough to feel the bottom layer changes.
3. Density is not resolvable but can be determined using regression formulas by Hamilton (1980).
4. Invert for attenuation using the modeled TL slopes. Center frequencies of each LFM sweep are to be used for the inversions. Vary attenuation values to obtain TL slopes and perform matched slope processing by comparing modeled TL slopes to the negative slope of 10log of measured energy.

### C. THIN LAYER INVERSION

The results from the sensitivity study proved that perturbations in two of the four candidate parameters, thin layer thickness and sound speed, resulted in appreciable changes in VLA pressure field differences. Therefore, only those two parameters could be inverted for using the acoustic pressure field as the base correlate input.

Since sound speed is a parameter in both layers of the bottom, it was necessary to find a frequency that was sensitive to sounds speed in the upper layer but not in the bottom. The lowest frequencies (50-125 Hz) showed sensitivity to sound speed in both layers and therefore could not be used. The mid/low frequencies (140-200 Hz) showed good sensitivity to thin layer sound speed, no sensitivity to the bottom sound speed and were sensitive to thin layer thickness. Because of this, it was necessary to process both parameters at the same time. This was the preferred bandwidth used for the thin layer inversion.

The modeled VLA pressure fields were created in a similar method used in the sensitivity study. However, for the inversion, actual bathymetry was used instead of a flat bottom (Wei, 2000). Since the inversion for the thin layer was attempting to discover

two parameters the model was executed a large number of times. Each thickness, from 2 to 20 meters, in one meter increments, varied over the full range of candidate sound speeds, from 1550 to 1650 m/s by 5 m/s increments. This procedure was performed for each frequency in the preferred bandwidth in 5 Hz intervals.

Observed data for the inversion was prepared in the manner described above for each discrete frequency to compare to its modeled counterpart. Although the movement of the ship in the time that it took for the J-15 to transmit from 50 to 200 Hz was minimal, and the distance traveled in a 5 Hz portion of that sweep was even smaller, it was critical to ensure accuracy of the field to be correlated. Any error in distance more than one wavelength produced significant degradation in the ambiguity surface. Results were very sensitive to distance.

Ambiguity surfaces (Figure 12) were produced according to the above matched field methodology using a linear processor. Each surface was then analyzed to determine the maximum correlate value and its corresponding sound speed and thin layer thickness. Surfaces with a maximum correlate of less than .35 were discarded as inaccurate. Those meeting the correlate criteria threshold were then averaged using the following weighted mean formula.

$$\prec c, h \succ = \sum \frac{w(c, h)}{\sum w},$$

where  $c$  and  $h$  are the best sound speed and thin layer thickness estimates from the ambiguity surface ensemble and  $w$  is the corresponding correlate peak value for each frequency meeting the .35 correlation criteria. Variance was calculated from the weighted mean value. Results showed the thin layer to have a sound speed of 1575.68 m/s and a standard deviation of 24.3 m/s. The thickness of the thin layer was 17.21 meters with a standard deviation of 3.26 meters.

It is worthy to note that ambiguity surfaces were produced for both coherent and non-coherent pressure fields. This was true for the sensitivity studies as well as the thin layer and bottom inversions. All graphics depicted in this paper are coherent. Surfaces constructed from magnitude only fields were too ambiguous to determine any of the parameters in question.

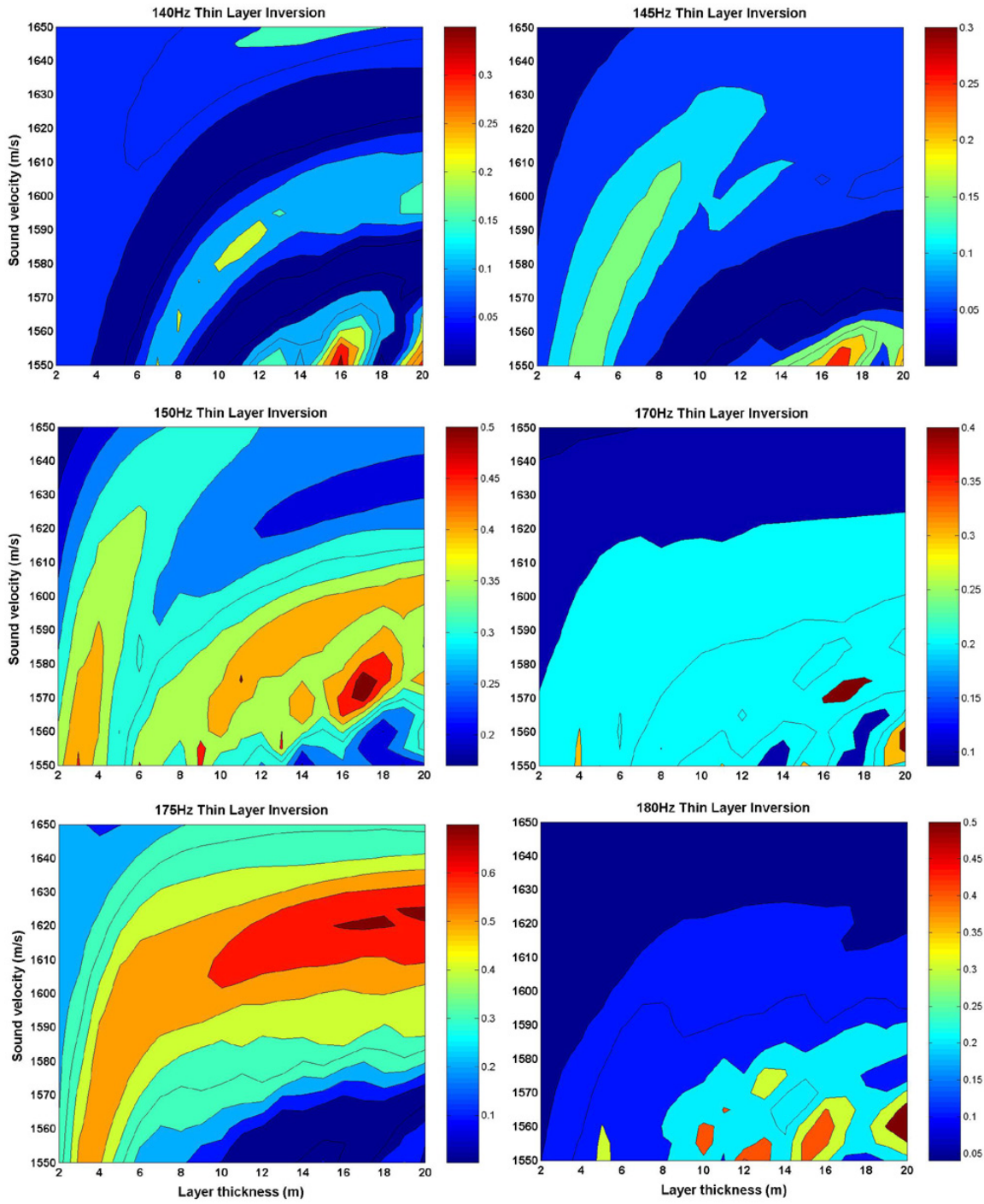


**Figure 12.** Thin layer ambiguity diagrams for both sound speed and layer thickness. Frequency increases from 140Hz at the top left to 180Hz at the bottom right. Frequency on diagrams increase left to right and top to bottom. Colorbars are not constant for each subplot with darkest red representing max correlation coefficient values for each diagram. Sound speed varies from 1550 to 1650 m/s while layer thickness ranges from 2 to 20 meters.

### C. BOTTOM LAYER INVERSION

As the bottom layer only had one invertible parameter, the complexity of the model data matrix was much simpler than the thin layer. The matrix was constructed with model runs between 1590 and 1730 m/s with 5 m/s increments. Observed data was built in the same manner as the thin layer inversion.

The frequency band used for the bottom inversion capped at 140 Hz based on lack of any sensitivity above that level. Frequencies below that level had varying degrees of sensitivity from 50-140Hz despite a clear diminishing sensitivity trend towards the high end of the bandwidth.

Since the model runs for this inversion took exponentially less time to complete, more runs could be completed inside the frequency band used. Model runs were performed at 65, 79, 81, 86, 92, 102, 105, 112, 129, 137, and 141 Hz. The larger number of runs allowed for greater statistical significance of results. The irregular frequency interval is due to a lack of observed signal to noise ratio in the observed data. When regular spacing was used, ambiguity diagram correlate values were often very low due to a low SNR at some frequencies. In order to rectify the SNR problem, individual data points were chosen visually from FFT spectral values of pulse compressed raw data (Figure 13).

Peak correlation values were chosen in the same method as the thin layer inversion except the threshold was .5 or higher. The same weighted sum was also employed. Sound speed in the lower layer was determined to be 1612.1 m/s with a sigma of 15.9 m/s (Figure 14).

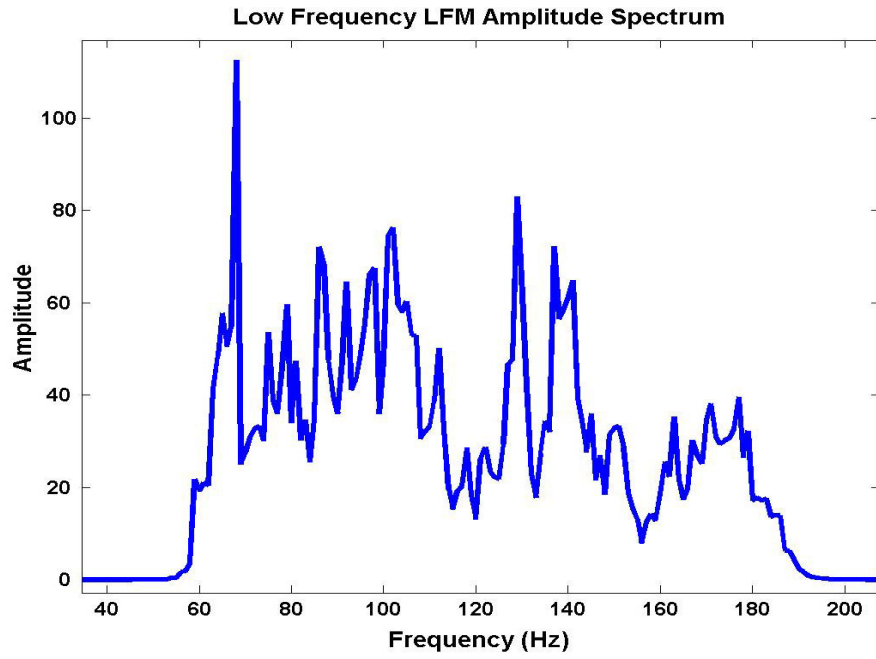


**Figure 13.** Low frequency LFM amplitude spectrum after pulse compression showing obvious peaks in SNR that were used for bottom sound speed inversion in Figure 13.

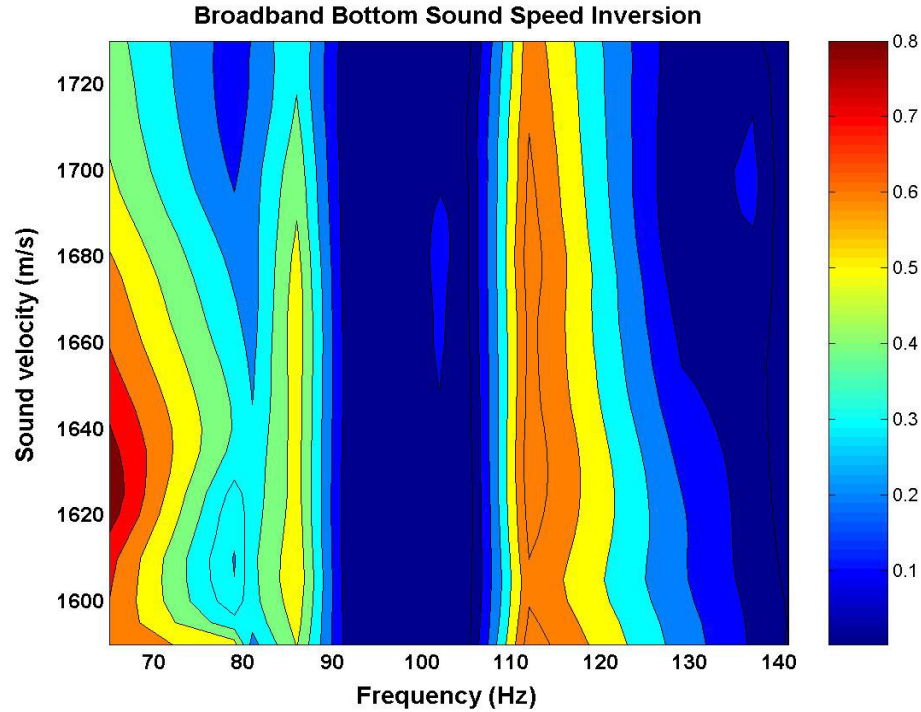


**Figure 14.** Bottom layer sound speed frequency dependent ambiguity diagram with sound speed ranging from 1590 to 1730 m/s. Highest correlation coefficients are depicted in reds and oranges and correspond to estimated sound speeds on y axis.

## D. ATTENUATION INVERSION

As noted in the sensitivity study, VLA pressure fields did not respond to an incremented increase or decrease of attenuation values and were therefore impossible to invert for using only vertical data.

The method that is valid and used here compared the slopes of the modeled depth integrated transmission loss (Figure 9) to the negative slope of  $10\log$  of depth integrated measured energy (Figure 15) gathered from observed data. Modeled absolute transmission loss could not be compared directly to the observational data as the source level from the experiment J-15 sound source was not known. The two slopes can be correlated via matched field processing after some minor manipulation. Transmission loss is defined as:

$$TL = -10 \log \frac{E}{E_0},$$

Measured energy is defined as:

$$L_e = 10 \log E$$

where  $E$  is the depth integrated energy and  $E_0$  is the reference energy. The slopes of the model  $TL$  and  $-L_e$  can be properly correlated to obtain high quality estimates of  $\alpha$ .

The modeled data vector ( $p^M$ ), which in this case consisted of multiple relative TL runs corresponding to increasing  $\alpha$  values, was formed from the output of a broadband TL calculator developed by Chiu (1996). The data inputs for the TL calculator used pressure vs. range outputs from the same broadband coupled-mode model used in the other inversions for consistency. It is noteworthy to mention that the normalization procedure must use the larger of the modeled and observed sum of squares to make sure this is a matched slope processor. The same linear MFP as before was used except  $p^o$  was replaced with  $-L_e$  and  $p^M$  was replaced with the modeled TL.

Peak correlation values pulled from the ambiguity diagrams (Figure 16.) produced by the matched field processor showed a non linear, frequency dependant attenuation (Figure 17).

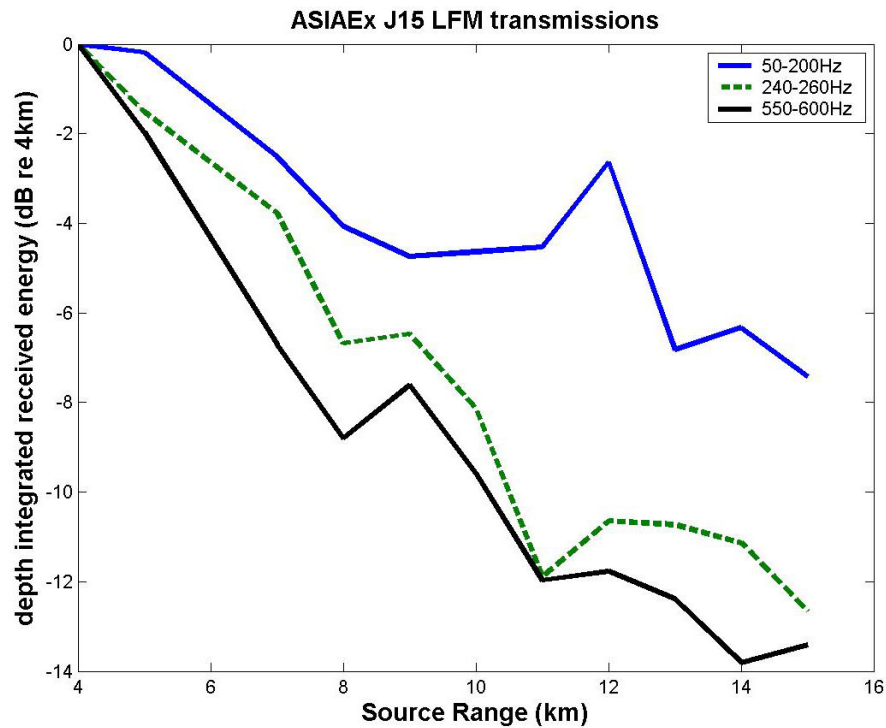


**Figure 15.** LFM measured negative energy ( $-10\log E$ ) slopes for low (50-200Hz), mid (240-260 Hz) and high (550-600 Hz) sweeps relative to energy at 4km.

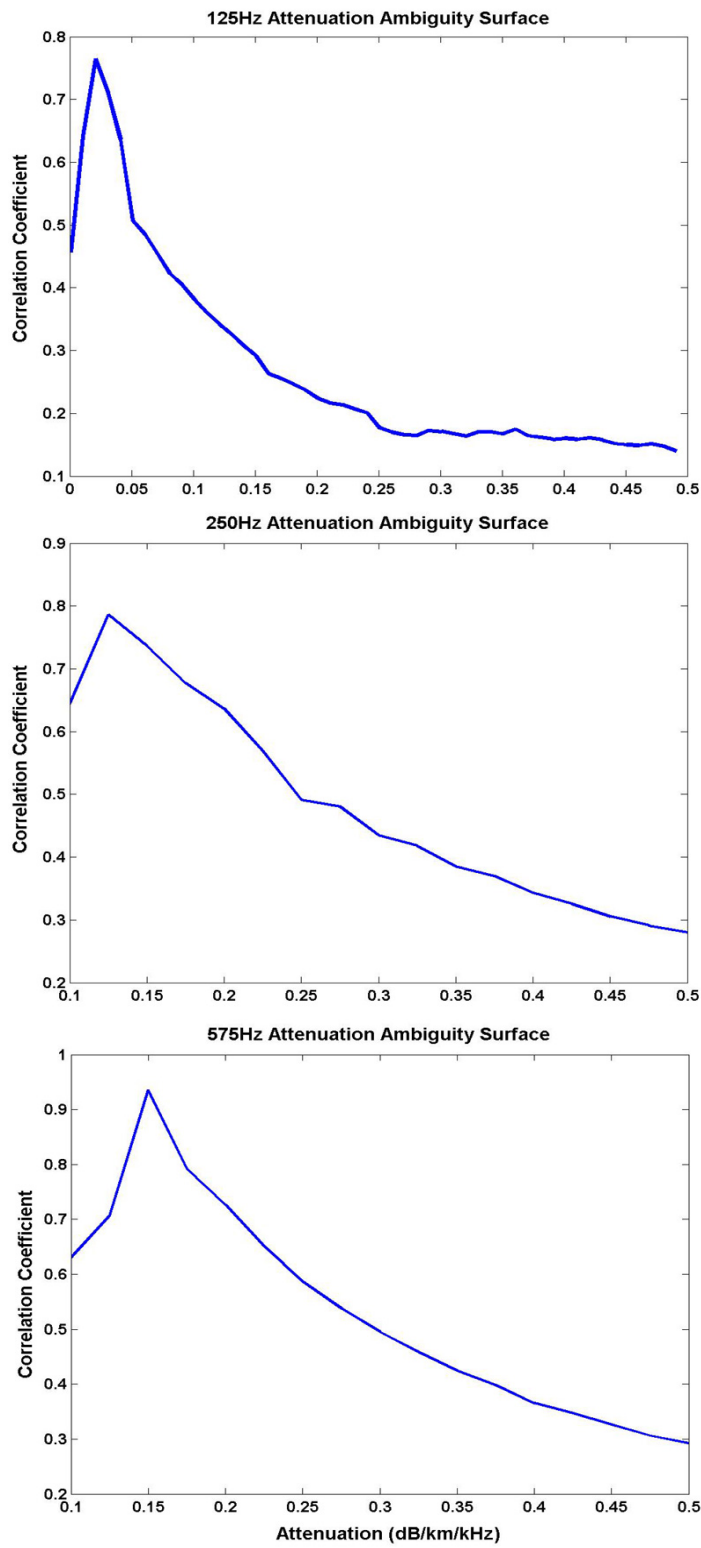


**Figure 16.** Attenuation ambiguity diagrams. Top subplot is for 125Hz, middle is 250Hz and bottom is 575Hz. X axis represents the attenuation value estimated from its corresponding TL slope. The y axis is the correlation coefficient value.

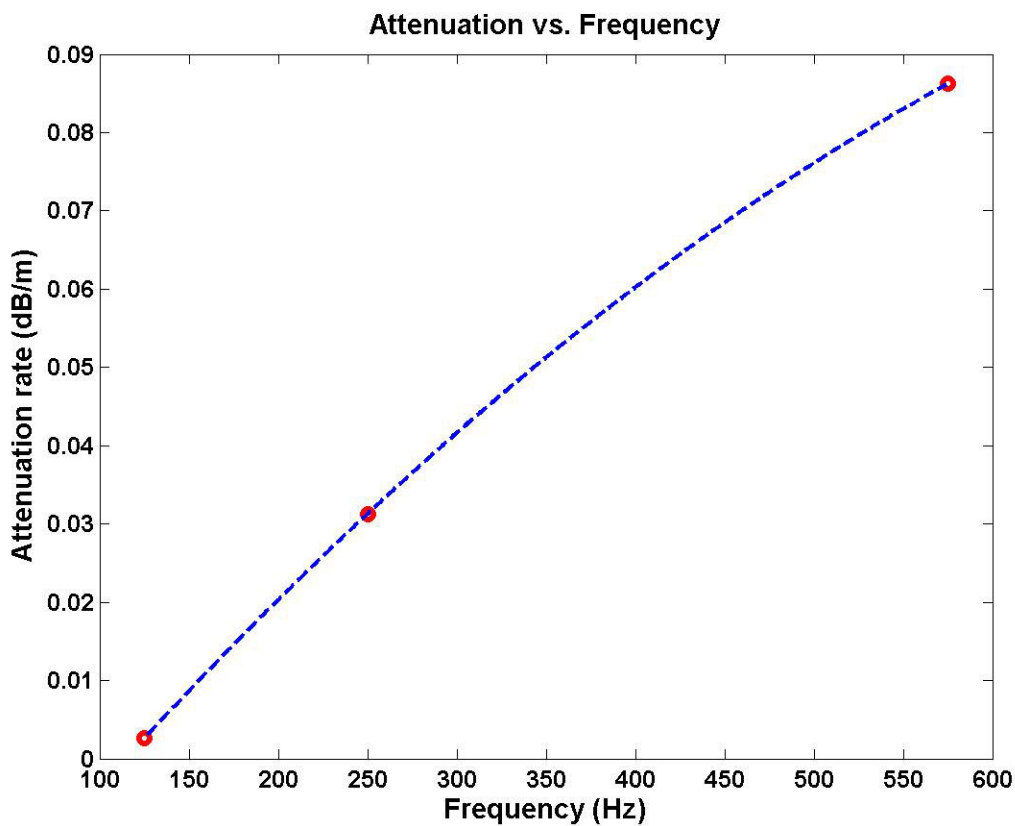


**Figure 17.** Attenuation rate versus frequency. Data set fit with a cubic spline curve.

THIS PAGE INTENTIONALLY LEFT BLANK

## IV. CONCLUSIONS

Data collected during ASIAEX and the corresponding sensitivity study produced excellent results and provided insight into techniques for future geoacoustic inversions. Results show that matched field processing alone is not adequate to properly characterize bottom parameters. Investigations into sensitivity of the parameters must accompany matched field processing prior to the inversion to understand resolvability and accuracy.

The sensitivity study produced one of the most important results of this thesis; the procedure describing the order to conduct the inversion is critical to obtaining efficient results. The sensitivity study also revealed the resolvability of the attenuation coefficient. Vertical pressure data is of no help to processing for attenuation. Horizontal data is useful and it can be estimated using matched field processing by matching the slopes of transmission loss to the negative slope of  $10\log$  of observed energy. Preliminary results also suggest that attenuation rate is not linear with frequency as previously thought (Hamilton, 2001). That study suggested that attenuation rate =  $\alpha f^1$ , regardless of sediment type. More research on this is recommended.

The chirp sonar data was the most compelling data source to determine the layering of the bottom model. It clearly showed two layers of sediment with a thin layer overlying a thicker layer. Due to the layering of the bottom, and the thickness of the thin layer approaching 20 meters, the bottom layer becomes acoustically unimportant at higher frequencies. Penetration is not deep enough to discern the bottom layer parameters.

This study focused on only one range (5km) from the experiment in order to invert for all of the parameters excluding attenuation which utilized horizontal received energy. Many more ranges could be explored as well as the all encompassing range dependent problem.

As the overall goal of this thesis was Naval warfighter support, one has to ask how a study of this nature is processed to reach the operational models of a sonar operator on a surface ship or submarine. The gap between the operational Navy and research community needs to be tightened. Onboard acoustic models in use today have

little valid bottom input for shallow water available to the operator. Studies like this one have the potential to aide in the improvement of future operational models.

## LIST OF REFERENCES

- Chiu, C.-S., Lynch, J.F., Ramp, S.R., Duda, T.F., Miller, C.W. and Tang, D., "Acoustic Intensity Fluctuations Induced by South China Sea Internal Tides and Solitons," IEEE J. Oceanic Eng., Vol 29, pp
- Ramp, S.R., Lynch, J.F, Dahl, P.H., Chiu, C.-S. and Simmen, J.A., "ASIAEX fosters advances in shallow water acoustics," EOS, Trans.AGU, vol.84, no. 37, pp. 361-367, 2003.
- Turgut, A, et al., "Inversion of range-dependent geoacoustic properties in South China Sea ASIAEx01 experimental site," J.Acoust. Soc. Am., Vol. 113, p.2218, 2003.
- Schock, S.C., "Remote prediction of the physical and acoustic properties of sediments in the South China Sea using a chirp sonar and biot theory," IEEE J. Oceanic Eng., Vol. 29, pp.XXX-XXX, Oct. 2004.
- Hamilton, E.L., "Geoacoustic modeling of the sea floor," J. Acoust. Soc. Am., Vol 68, pp 1313-1340, 1980.
- Hamilton, E.L., "Sound velocity-density relations in sea-floor sediments and rocks," J. Acoust. Soc. Am., Vol 63, pp 366-377, 1978.
- Lin, Y.-T., et al., "An estimate of the bottom compressional wave speed profile in the northeastern South China Sea using sources of opportunity," IEEE J. Oceanic Eng., special issue on Asian marginal seas, 2004.
- Chiu, C.-S., Miller, J.H. and Lynch, J.F., "Forward coupled-mode propagation modeling for coastal acoustic tomography," J. Acoust. Soc. Amer., Vol. 99, pp 793-802, 1996.
- Tolstoy, A., "Match Field Processing for Underwater Acoustics," (World Scientific, NJ, 1993).
- Wei, R.-C., "Bathymetric survey in South China Sea for ASIAEX," Inst. Undersea Technol., National Sun Yat-Sen Univ., Cruise Rep, June 2000.

THIS PAGE INTENTIONALLY LEFT BLANK

## **INITIAL DISTRIBUTION LIST**

1. Defense Technical Information Center  
Ft. Belvoir, Virginia
2. Dudley Knox Library  
Naval Postgraduate School  
Monterey, California
3. James Lynch  
Woods Hole Oceanographic Institution  
Woods Hole, MA
4. Steve Ramp  
Naval Postgraduate School  
Monterey, California
5. Ellen Livingston  
Office of Naval Research  
Arlington, VA
6. Ching-Sang Chiu  
Naval Postgraduate School  
Monterey, California
7. Chris Miller  
Naval Postgraduate School  
Monterey, California
8. John Marburger  
Joint Typhoon Warning Center  
Pearl Harbor, HI